GEOPHYSICS, VOL. 74, NO. 1 (JANUARY-FEBRUARY 2009); P. N15–N23, 6 FIGS., 3 TABLES.
10.1190/1.3026620

Low-frequency reflections from a thin layer with high attenuation caused by interlayer flow

Beatriz Quintal[1], Stefan M. Schmalholz[1], and Yuri Y. Podladchikov[2]

ABSTRACT

The 1D interlayer-flow (or White's) model is based on Biot's theory of poroelasticity and explains low-frequency seismic wave attenuation in partially saturated rocks by wave-induced fluid flow between two alternating poroelastic layers, each saturated with a different fluid. We have developed approximate equations for both the minimum possible value of the quality factor, Q, and the corresponding fluid saturation for which Q is minimal. The simple approximate equations provide a better insight into the dependence of Q on basic petrophysical parameters and allow for a fast assessment of the minimal value of Q. The approximation is valid for a wide range of realistic petrophysical parameter values for sandstones partially saturated with gas and water, and shows that values of Q can be as small as two. We applied theinterlayer-flow model to study the reflection coefficient of a thin (i.e., between 6 and 11 times smaller than the incident wavelength) layer that is partially saturated with gas and water. The reflection coefficient of the layer, caused only by a contrast in attenuation between the layer and the nonattenuating background medium, can be larger than 10% for $Q < 4$ within the layer. The reflection coefficient was calculated with finite difference simulations of wave propagation in heterogeneous, poroelastic solids and in equivalent viscoelastic solids. The reflection coefficient of the layer is also estimated with an analytical solution using a complex velocity for the layer. The numerical and analytical results agree well. Our results indicate that reflection coefficients of gas reservoirs can be significantly increased and frequency dependent in the low-frequency range because of attenuation within the reservoir caused by wave-induced flow.

INTRODUCTION

Because the exploration industry continues efforts to extend the bandwidth of the seismic experiment, it is imperative to understand the reflectivity structure of the subsurface at low frequencies. Rock physics models indicate that partially saturated reservoirs can exhibit high attenuation and dispersion characteristics at frequencies less than about 10 Hz (e.g., White et al., 1975; Pride et al., 2004; Toms et al., 2006; Carcione, 2007). High attenuation (or low-quality factor, Q) contrast can significantly increase the reflection coefficient at a boundary, which has been shown by analytical (e.g., Bourbié et al., 1987), numerical (e.g., Ganley, 1981; Bourbié and Gonzalez-Serrano, 1983; Carcione et al., 1998), and laboratory (e.g., Bourbié and Nur, 1984) studies. The implication is that the low-frequency reflectivity structure of the subsurface may be significantly different than that encountered thus far in seismic experiments. The additional reflectivity of porous rocks with multiphase fluid content (as opposed to those fully saturated with water), because of attenuation, can significantly increase the amplitude of reflections of hydrocarbon reservoirs. Attenuation-dominated reflection coefficients can even lead to significant reflectivity when there is no acoustic impedance contrast between a reservoir and the surrounding country rock, and when the wavelengths of the seismic waves are much greater than the thickness of the reservoir.

High values of attenuation in hydrocarbon reservoirs have often been observed (e.g., Klimentos, 1995; Dasgupta and Clark, 1998; Rapoport et al., 2004; Maultzsch et al., 2003), and related reflections in the low-frequency range have recently attracted an increased interest in the scientific and industrial communities. Chapman et al. (2006) remark that hydrocarbon reservoirs often show abnormally high attenuation in the low-frequency range. Goloshubin et al. (2006) use some examples of field-data processing to show that oil-rich reservoirs exhibit increased reflective properties at low frequencies, and that expanding the active seismic bandwidth to low fre-

Manuscript received by the Editor 7 May 2008; revised manuscript received 8 August 2008; published online 17 December 2008.
[1]ETH Zurich, Geological Institute, Zurich, Switzerland. E-mail: beatriz.quintal@erdw.ethz.ch; stefan.schmalholz@erdw.ethz.ch.
[2]University of Oslo, Physics of Geological Processes, Oslo, Norway. E-mail: iouri.podladchikov@fys.uio.no.

quencies has a strong potential for predicting fluid content. Korneev et al. (2004) observed in both laboratory and field data that phase delay associated with high attenuation allows increased reflectivity from thin layers at the low-frequency end of the spectra.

The major cause of seismic attenuation in porous media in the low-frequency range is presumably wave-induced fluid flow on the mesoscopic scale, i.e., the scale much larger than the pore size but much smaller than the wavelength (e.g., White et al., 1975; Pride et al., 2004; Toms et al., 2006). Attenuation and velocity dispersion can be explained by the combined effect of mesoscopic-scale inhomogeneities and energy transfer between wave modes (conversion of fast P-wave to slow P-wave). If the compressibility of the fluids varies significantly in that scale, the flow of pore fluids between different regions can be important at low (seismic) frequencies (e.g., 1 to 10 Hz). White (1975) and White et al. (1975) were the first to introduce the mesoscopic-loss mechanism providing a physically based model for low-frequency wave attenuation. White (1975) presents a 3D model considering gas pockets in a water-saturated porous medium. White et al. (1975) present a 1D version of the 3D model, referred to as the interlayer-flow model. The analytical solution of White's model yields the velocity dispersion and the frequency-dependent quality factor, Q, for a given set of rock properties. Dutta and Odé (1979a, b) and Dutta and Seriff (1979) solve the problem exactly by using Biot's theory (Biot, 1962) and confirm White's results. They show that wave-induced flow of the pore fluid can be modeled using Biot's equations of poroelasticity (Biot, 1962) with spatially varying petrophysical parameters. Several laboratory experiments with porous rocks provided evidence of the existence of mesoscopic saturation heterogeneities (Murphy, 1984; Cadoret et al., 1995, 1998).

In this study, we use the 1D interlayer-flow model (White et al., 1975; Carcione and Picotti, 2006) to investigate if attenuation in a reservoir can be high enough so that the reflection coefficient of a thin reservoir layer caused only by attenuation can be significant, i.e., larger than 5%. The first aim of this study is to derive a simple, approximate equation to calculate the minimum value of Q for a few realistic petrophysical parameter values for a homogeneous rock partially saturated with water and gas. To do so, we group the petrophysical parameters, required by the analytical solution of the 1D interlayer-flow model, into two subsets: s and g. One group of petrophysical parameters, s (dominated by the flow parameters, viscosity and permeability), controls the transition frequency f_{tr} at which the minimum value of Q is achieved; and the other group, g (consisting mostly of elastic moduli and porosity), dominates the calculation of the value of the minimum Q. Using the approximate equation, we are able to quickly calculate lower bounds of Q for realistic earth parameters. The second aim of this work is to quantify the reflection coefficient of a thin (compared to the wavelength) attenuating layer representing a reservoir and exhibiting a small value of Q caused by interlayer flow. We study the reflection coefficient of a thin layer having high attenuation but no (real part of) acoustic-impedance contrast with the surrounding background medium with: (1) finite-difference modeling of wave propagation in a heterogeneous poroelastic medium (Biot's equations), (2) finite-difference modeling of wave propagation in an equivalent viscoelastic medium, and (3) an analytical solution for the reflection coefficient of a thin elastic layer using a complex P-wave velocity for the layer.

We start with a description of the interlayer-flow model and the derivation of a new approximation for the minimum value of the quality factor, $Q_{\min}$. Next, dispersion and attenuation resulting from interlayer flow are approximated with an equivalent viscoelastic model. Afterward, numerical simulations and an analytical solution are used to quantify the reflection coefficient from a thin layer because of attenuation contrast caused by interlayer flow and viscoelasticity.

THE ANALYTICAL SOLUTION OF WHITE'S MODEL

In the 1D interlayer-flow model (e.g., White et al., 1975; Norris, 1993; Carcione and Picotti, 2006), a partially saturated reservoir is represented by a laminated solid made of two periodically alternating layers of media 1 and 2. Each medium is a fully saturated poroelastic solid that differs by the pore fluid properties, here alternating water and gas saturation. Recent detailed descriptions of the 1D interlayer-flow model can be found in Carcione and Picotti (2006) and Carcione (2007). Attenuation and the associated dispersion of the phase velocity are caused by wave-induced viscous (dissipative) fluid flow, generated by fluid pressure differences between the layers. The analytical solution for the interlayer-flow model yields the frequency-dependent quality factor Q and phase velocity V_P for a given set of rock properties (White et al., 1975; Carcione and Picotti, 2006). Q and V_P are given by

$$Q = \frac{\mathrm{Re}(E)}{\mathrm{Im}(E)}, \tag{1}$$

$$V_P = \left(\mathrm{Re}\left(\frac{1}{V}\right)\right)^{-1}, \tag{2}$$

where E is the complex modulus for a P-wave traveling along the direction perpendicular to the layering, also called plane-wave modulus, and V is the complex velocity, or

$$V = \sqrt{\frac{E}{\rho}}, \tag{3}$$

where ρ is the bulk density of the partially saturated poroelastic medium. We rearrange the equations of the analytical solution for the frequency-dependent quality factor Q given by Carcione and Picotti (2006). To better understand the controlling parameters, we begin by defining the complex modulus E as the product of a real number E_0 and a complex number, b,

$$E = E_0 b, \tag{4}$$

where

$$E_0 = \left(\frac{p_1}{E_{G1}} + \frac{p_2}{E_{G2}}\right)^{-1} \tag{5}$$

and

$$b = (1 + (I_1 g_1 + I_2 g_2)^{-1})^{-1}, \tag{6}$$

so that we obtain the equation

$$Q = \frac{\mathrm{Re}(b)}{\mathrm{Im}(b)}. \tag{7}$$

The indexes 1 and 2 refer to the two different porous media, i.e., the two periodically alternating layers. For each saturated porous medium ($j = 1,2$)

$$g_j = \frac{K_{Ej}}{2E_0(r_2 - r_1)^2 p_j}, \tag{8}$$

$$I_j = \sqrt{i\omega s_j}\coth\left(\frac{i\omega s_j}{2}\right), \tag{9}$$

and

$$s_j = \frac{\eta_j d_j^2}{K_{Ej}k_j}. \tag{10}$$

The quality factor Q (equation 7) was written as a function of two groups of petrophysical parameters, s and g, and the angular frequency, $\omega(=2\pi f)$. Table 1 shows the symbols used for the basic petrophysical parameters mentioned in this paper, and all remaining parameters are defined below, with the index j omitted for clarity

$$p = \frac{d}{d_1 + d_2}, \tag{11}$$

where d is the thickness of the layer, and the normalized layer thickness p represents the saturation of the corresponding fluid in the partially saturated reservoir. The plane-wave modulus of the saturated rock is

$$E_G = K_G + \frac{4}{3}\mu_m, \tag{12}$$

an effective modulus is

$$K_E = \frac{E_m M}{E_G}, \tag{13}$$

the ratio of fast P-wave fluid tension to total normal stress is

$$r = \frac{\alpha M}{E_G}, \tag{14}$$

Table 1. Symbols used for the basic petrophysical parameters.

Symbol	Parameter
ϕ	Porosity
K_m	Bulk modulus of the dry frame
μ_m	Shear modulus of the dry frame
K_s	Bulk modulus of the grain
μ_s	Shear modulus of the grain
K_f	Bulk modulus of the fluid
η	Viscosity
k	Permeability
ρ_s	Density of the grain
ρ_f	Density of the fluid

the Gassmann modulus is

$$K_G = K_m + \alpha^2 M, \tag{15}$$

the dry-rock fast P-wave modulus is

$$E_m = K_m + \frac{4}{3}\mu_m, \tag{16}$$

the solid-grain bulk modulus is

$$M = \left(\frac{\alpha - \phi}{K_s} + \frac{\phi}{K_f}\right)^{-1}, \tag{17}$$

and

$$\alpha = 1 - \frac{K_m}{K_s}. \tag{18}$$

The subscripts m stands for matrix (or dry frame), s and f for solid and fluid constituents, respectively, G for Gassmann, and E for effective. Equation 12 gives the low-frequency plane-wave modulus when the bulk modulus of the fluid is averaged according to Gassmann-Wood's law, and equation 5 gives the high-frequency plane-wave modulus, according to Gassmann-Hill's law (e.g., Mavko et al., 1998; Carcione and Picotti, 2006; Toms et al., 2006).We present here a modified form of the equation for Q (equation 7) by only rearranging E in equation 4 to express Q as a function of two petrophysical parameter groups, g and s, and the angular frequency ω. The parameter s (equation 10) is dominated by the flow parameters, viscosity and permeability, and g (equation 8) consists mostly of elastic moduli and porosity. The frequency-dependent parameter Q has always a minimum at a certain frequency, referred to here as transition frequency, f_{tr}. An approximation for f_{tr} was given by Dutta and Seriff (1979) for a rock partially saturated with water and gas (i.e., one fluid compressibility much smaller than the other):

$$f_{tr} \approx \frac{8k_1 K_{E1}}{\pi\eta_1 d_1^2} = \frac{8}{\pi s_1}, \tag{19}$$

where index 1 refers to the water-saturated layer. The transition frequency is a function of the parameter s, which is one of the two petrophysical parameter groups introduced above when decomposing the analytical solution for Q. In the following section, we consider only the value of Q at the transition frequency, which is minimal with respect to all frequencies but can still vary significantly with varying petrophysical parameters. With further insight into the expression for Q (equation 7), we provide here an approximate equation for the minimum value of Q with respect to the petrophysical parameters (always at the transition frequency), referred to here as $Q_{\min}$.

The approximation for $Q_{\min}$

The analytical solution of the interlayer-flow model (equations 1–18) yields Q (equation 1 or 7) as a complicated function of petrophysical parameters, and it is not straightforward to evaluate the influence of each one on the attenuation of a partially saturated rock (Carcione and Picotti, 2006). It is therefore difficult to evaluate how small the value of Q can be for a partially saturated reservoir rock in the low-frequency range. For a sinusoidal motion in a standard linear solid, or a Zener (1948) viscoelastic material, the minimum quality factor $Q_{\min}$ at the transition frequency can be approximated by (e.g., Liu et al., 1976; Mavko et al., 1998)

$$Q_{\min} = \left(\frac{\mathrm{Re}(E)}{\mathrm{Im}(E)}\right)_{\min} \approx \frac{2\sqrt{E^H E^W}}{E^H - E^W}, \quad (20)$$

where E^W and E^H are the low- and high-frequency limits of the complex modulus E. At those limits, the modulus E becomes real and independent of frequency, and thus the material behaves elastically. If we assume that the frequency-dependent behavior of Q in a Zener viscoelastic material is similar to the frequency-dependent behavior of Q in the interlayer-flow model, we can use saturation averaging for calculating E in the low- and high-frequency limits, i.e., Gassmann-Wood and Gassmann-Hill limits, respectively (e.g., Mavko et al., 1998; Toms et al., 2006). This indicates that the value of $Q_{\min}$ is independent of the ratio η/k, which is only part of the parameter s (equation 10) but not present in the Gassmann-Wood and Gassmann-Hill limits (equations 12 and 5, respectively). We therefore tested the dependence of $Q_{\min}$ on s using the analytical solution (equations 4–18). We used typical parameters for reservoir rocks having partial water/gas saturation (Table 2) and varied the rock parameters independently within a realistic range (e.g., K_s from 25 to 40 GPa, ϕ from 0.1 to 0.3, and d_1 from 0.1 m to 1 m). We found that the variation of $Q_{\min}$ with s is indeed negligible. Instead, the amplitude of $Q_{\min}$ is effectively a linear function of only g (equation 8), or more precisely, the sum $g_1 + g_2$ (Figure 1)

$$Q_{\min} \approx 1.3 + 4.9(g_1 + g_2). \quad (21)$$

This approximation indicates that the value of $Q_{\min}$ should never be smaller than 1.3 because the parameter $g_1 + g_2$ is always positive. The approximation also gives the order of magnitude of the minimum value of $Q_{\min}$ that can be expected for the interlayer-flow model for typical reservoir rocks having partial water/gas saturation.

However, $Q_{\min}$ is still a complicated function of several basic petrophysical parameters, for example K_s, K_f, p, and ϕ, and we seek a simpler estimate for $Q_{\min}$. Using equations 8 and 11,

$$g_1 + g_2 = \frac{1}{2E_0(r_2 - r_1)^2}\left(\frac{K_{E1}}{p_1} + \frac{K_{E2}}{p_2}\right). \quad (22)$$

We define the patch-size or saturation ratio

$$p_r = p_2/p_1, \quad (23)$$

and substitute equations 5 and 23 in equation 22

$$g_1 + g_2 = \frac{1}{2(r_2 - r_1)^2}\left(K_{E1} + \frac{K_{E2}}{p_r}\right)\left(\frac{1}{E_{G1}} + \frac{p_r}{E_{G2}}\right). \quad (24)$$

Because of the linear dependence in equation 21, $Q_{\min}$ is minimal if $g_1 + g_2$ is minimal. Inspecting equation 24, we see that $g_1 + g_2$ must have a minimum for a certain value of p_r which can be determined by setting the derivative of $g_1 + g_2$ with respect to p_r to zero:

$$\frac{d}{dp_r}(g_1 + g_2) = 0. \quad (25)$$

Solving equation 25 for p_r, we find the optimal patch-size ratio (or optimal saturation ratio) that minimizes $g_1 + g_2$,

$$p_r^{\min} = \sqrt{\frac{E_{G2}K_{E2}}{E_{G1}K_{E1}}}. \quad (26)$$

Substituting equation 26 in equation 24, we eliminate the geometrical (or saturation) parameter involved in the formula for $Q_{\min}$ (equations 21 and 24)

$$g_1 + g_2 = \frac{1}{2(r_2 - r_1)^2}\left(\sqrt{\frac{K_{E1}}{E_{G1}}} + \sqrt{\frac{K_{E2}}{E_{G2}}}\right)^2. \quad (27)$$

In addition, we want the approximation for $Q_{\min}$ (equation 21), for typical reservoir rocks with partial water/gas saturation, expressed in terms of the basic petrophysical parameters. We substitute the definitions of E_G, K_E, r, and M (equations 12–14 and 17) in equation 27. We make the approximation $M_2 = 0$, based on the fact that $K_{f2} \ll K_{f1}$, for gas/water saturation. Then $g_1 + g_2$ can be approximated as

$$g_1 + g_2 \approx q = \frac{\left(\frac{K_m}{K_s} + \frac{4\mu_m}{3K_s}\right)\left(1 - \phi + \frac{\phi K_s}{K_{f1}} - \frac{K_m}{K_s}\right)}{2\left(1 - \frac{K_m}{K_s}\right)}. \quad (28)$$

The approximate parameter q is a function of the four parameters K_m/K_s, μ_m/K_s, K_{f1}/K_s, and ϕ. The ratios K_m/K_s and μ_m/K_s are related

Table 2. Petrophysical parameters used in this study. See Table 1 for definition of the symbols.

	Water-saturated sandstone	Gas-saturated sandstone	Background medium
K_s (GPa)	37	37	8
μ_s (GPa)	44	44	6
ρ_s (kg/m^3)	2650	2650	1800
ϕ	0.3	0.3	0.01
K_f (GPa)	2.4	0.022	2.4
ρ_f (kg/m^3)	1000	100	1000
η (Pa s)	0.001	10^{-5}	0.001

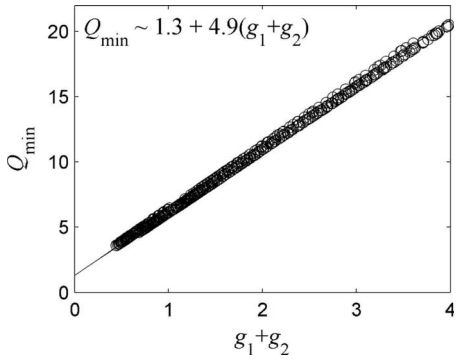

Figure 1. Exact values of $Q_{\min}$ (the circles) calculated using the analytical solution of White's interlayer-flow model for a wide variation of realistic parameters for reservoir rocks having partial gas/water saturation (Table 2) as a function of the parameter $g_1 + g_2$ (equation 22). The approximately linear variation of $Q_{\min}$ with the value of $g_1 + g_2$ is fitted accurately with the straight solid line.

to the degree of consolidation of the rock (see next section), and the ratio K_{f1}/K_s expresses the bulk modulus ratio of fluid (water) and solid constituents. Using q, we fit the analytical value of $Q_{\min}$ with (Figure 2)

$$Q_{\min} \approx 1.8 + 6.3q. \quad (29)$$

Application of the approximation for $Q_{\min}$

The approximate value of $Q_{\min}$ (equation 29) for a reservoir rock with partial water/gas saturation is a function of the four parameters K_m/K_s, μ_m/K_s, K_{f1}/K_s, and ϕ. However, the parameters K_m and μ_m are related to K_s and μ_s, respectively, through ϕ. There are empirically derived equations for those relations in the literature (e.g., Krief et al., 1990; Pride, 2003). We use here Pride's (2003) equations:

$$K_m = K_s(1 - \phi)/(1 + c\phi), \quad (30)$$

$$\mu_m = \mu_s(1 - \phi)/(1 + 3c\phi/2). \quad (31)$$

The parameter c is related to the degree of consolidation between grains and the greater it is, the less consolidated the rock is. The parameter c is considered to vary between two and 20 for consolidated sandstones (Pride, 2003), but values of K_s, K_m, and ϕ found in the literature provide values of c about 40 and larger (e.g., Müller and Gurevich, 2005; Carcione and Picotti, 2006).

We fix the values for K_s, K_{f1}, and μ_s (Table 2, sandstone parameters) and calculate the value of $Q_{\min}$ (with equation 29) in the space K_m/K_s versus ϕ (Figure 3a). We apply Pride's relations to evaluate if our independent variation of the two parameters K_m/K_s and ϕ generates acceptable values of c for reservoir rocks. We therefore plot the value of c, calculated from equation 30, also in the space K_m/K_s versus ϕ (Figure 3b). We consider here values of c as being acceptable (or realistic) if they are between two and 40. Figure 3b shows that nonacceptable values (i.e., $c > 40$) only occur in a small area for small values of both K_m/K_s and ϕ. The contour line specifying $c = 40$ is also plotted in Figure 3a to indicate the area of values of $Q_{\min}$ corresponding to acceptable values of c. Values of $Q_{\min}$ can be as small as two for the petrophysical parameter values considered (Figure 3a). For the applied values, the optimal patch-size or saturation ratio (equation 26) is about 0.11, corresponding to about 9% gas saturation (equation 23). Figure 3a shows that the smallest values of $Q_{\min}$ occur for high values of c corresponding to less consolidated rocks (according to Pride, 2003). The error of the approximated value of $Q_{\min}$ (equation 29) with respect to the exact value calculated with the analytical solution of the 1D interlayer-flow model (equation 1) is shown in Figure 3c, and we see that for realistic values of c, it is smaller than 5%. The error is calculated using the values of K_s, K_{f1}, and μ_s given in Table 2. A further variation of the values of K_s and μ_s within one order of magnitude, and a variation of K_{f1} and K_{f2} within a factor of two, provide approximations of $Q_{\min}$ (equation 29) that are still accurate within 10%, compared to the full analytical solution (equation 1). We therefore consider equation 29 a good approximation for most sandstones partially saturated with water and gas.

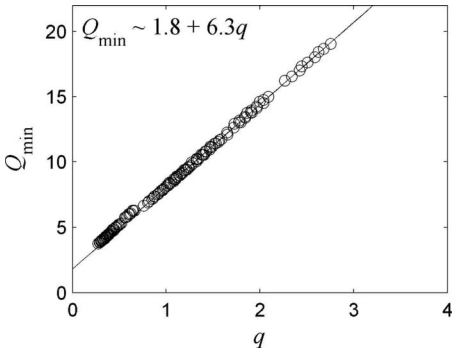

Figure 2. Exact values of $Q_{\min}$ (the circles) calculated using the analytical solution of White's interlayer-flow model for a wide variation of realistic parameters for reservoir rocks having partial gas/water saturation (Table 2) as a function of the parameter q (equation 28). The parameter q is much simpler than the parameter $g_1 + g_2$ used in Figure 1. The approximately linear variation of $Q_{\min}$ with the value of q is fitted accurately with the straight solid line.

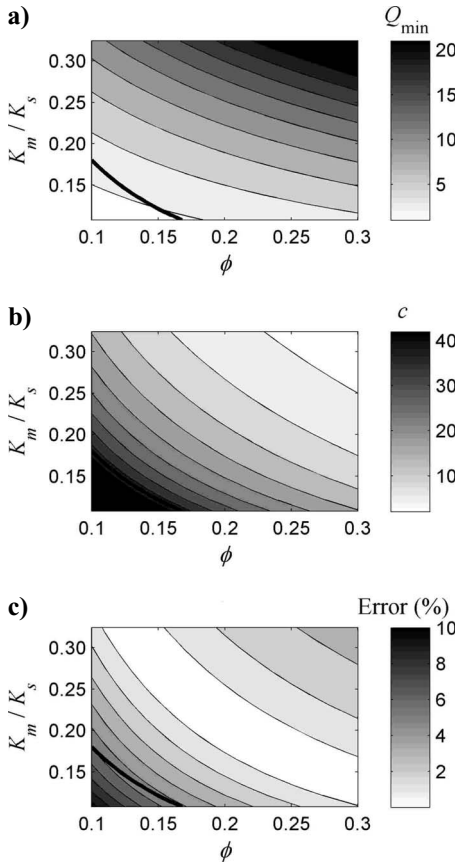

Figure 3. Contour plots of (a) $Q_{\min}$ (equation 29), (b) the corresponding value for c (equation 30), and (c) the corresponding error of $Q_{\min}$ with respect to the exact analytical solution, all in the space K_m/K_s versus ϕ. For calculating the value of $Q_{\min}$, the parameters K_s, K_{f1}, and μ_s are fixed and given in Table 2. The parameter c is the consolidation parameter (equations 30 and 31; Pride, 2003). Pride's relations are used to evaluate if the independent variation of the two parameters, K_m/K_s and ϕ, generates acceptable (realistic) values of c for reservoir rocks (i.e., between 2 and 40). The bold contour line in (a) and (c) corresponds to $c = 40$ and realistic values of c occur above this line as shown in (b). $Q_{\min}$ can be as small as two for $c < 40$. The error of $Q_{\min}$ in (c) is the absolute value of the difference between the approximated (equation 29) and the exact analytical values of $Q_{\min}$, divided by the exact analytical value.

EQUIVALENT VISCOELASTIC MODEL

We use the Zener or standard linear solid model (Zener, 1948) for a viscoelastic solid to simulate an equivalent attenuation around the transition frequency in the reservoir, as the one provided by the interlayer-flow model. The stress-strain relation for such viscoelastic model is (e.g., Carcione, 2007)

$$\tau + \gamma_\tau \frac{\partial \tau}{\partial t} = E_R\left(\varepsilon + \gamma_\varepsilon \frac{\partial \varepsilon}{\partial t}\right), \tag{32}$$

where τ is stress, ε is strain, E_R is the relaxed modulus (obtained for $\omega = 0$), and γ_τ and γ_ε ($\gamma_\varepsilon \geq \gamma_\tau$) are the relaxation times. These parameters are related to the properties of the three rheological elements (elasticity of the two springs and viscosity of the dashpot) of the viscoelastic model (e.g., Carcione, 2007). The frequency-dependent complex modulus, $E(=\tau/\varepsilon)$, is obtained by performing a Fourier transform of equation 32, and

$$E = E_R\left(\frac{1 + i\omega\gamma_\varepsilon}{1 + i\omega\gamma_\tau}\right). \tag{33}$$

We calculate the parameters E_R, γ_τ, and γ_ε for a specific mechanical model that approximately fits the attenuation/dispersion behavior of the interlayer-flow model. We use the values of the minimum quality factor ($Q_{\min}$), transition frequency (f_{tr}), and P-wave velocity at the low-frequency Gassmann-Wood limit (V_P^W, where the superscript W stands for Wood) of the interlayer-flow model to calculate these parameters. The values of γ_τ and γ_ε are calculated by solving two equations for $Q_{\min}$ and f_{tr} (Liu et al., 1976; Carcione, 2007)

$$Q_{\min} = 2\sqrt{\gamma_\varepsilon \gamma_\tau}/(\gamma_\varepsilon - \gamma_\tau), \tag{34}$$

$$f_{tr} = 1/(2\pi\sqrt{\gamma_\varepsilon \gamma_\tau}), \tag{35}$$

and E_R is calculated from

$$V_P^W = \sqrt{E_R/\rho}, \tag{36}$$

where the P-wave velocity at the low-frequency limit (V_P^W) is calculated using the Gassmann-Wood formula for averaging saturation heterogeneities (Mavko et al., 1998; Toms et al., 2006) and ρ is the bulk density of the partially saturated poroelastic medium, or the density of the equivalent viscoelastic medium

$$\rho = (1 - \phi)\rho_s + \phi\rho_f. \tag{37}$$

Once the parameters E_R, γ_τ, and γ_ε are known, the complex modulus, E, of the equivalent viscoelastic model can be calculated from equation 33, and then the frequency-dependent Q and V_P, using equations 1–3. The frequency-dependent quality factor and P-wave velocity of the partially saturated porous material (analytical solution of interlayer-flow model) and of the equivalent viscoelastic material are shown in Figure 4. We used the parameters of a gas- and water-saturated sandstone, given in Table 2, with $c = 38$ and $k = 170$ mD, to calculate the curves shown in Figure 4. Those physical parameters provide $Q_{\min} = 4.2$ and $f_{tr} = 6.5$ Hz. For the equivalent viscolastic model, we use the approximations given by equations 29 and 19, and the Gassmann-Wood formula to calculate the input $Q_{\min}$, f_{tr}, and V_P^W, respectively. At frequencies higher than f_{tr}, we observe a difference between the curves plotted using the analytical solution of the interlayer-flow model and the equivalent viscoelastic model. This difference occurs because the value of Q for the viscoelastic model is proportional to the frequency (which can be observed in equation 33), whereas the value of Q for the interlayer-flow model is proportional to the square root of the frequency (compare equation 9). Those differences are smaller than 5% for the P-wave velocity and 25% for the quality factor if the frequencies are not larger than four times the transition frequency. Because we are interested here only in frequencies closely around the transition frequency, this viscoelastic approach yields a reasonably accurate approximation of the quality factor for the purpose of our numerical simulations.

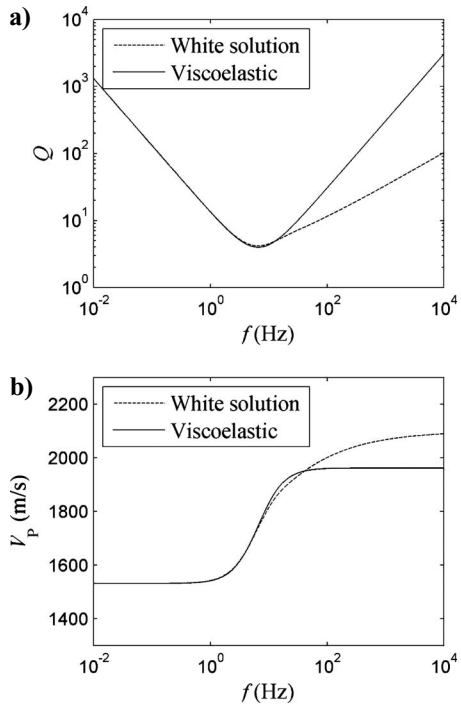

Figure 4. (a) Frequency-dependent quality factor, Q, and (b) P-wave velocity, V_P, versus frequency. Q and V_P are calculated by the analytical solution of the interlayer-flow model (White's solution) and the equivalent viscoelastic model (equations 32–36). The petrophysical parameters are for gas- and water-saturated sandstone (Table 2), $c = 38$, $k = 170$ mD, and the saturations have been calculated with equation 26, providing about 9% gas saturation. For this set of parameters, the transition frequency is $f_{tr} = 6.5$ Hz and the minimum value of Q is $Q_{\min} = 4.2$.

QUANTIFICATION OF REFLECTION COEFFICIENT

We performed numerical simulations for seven different sets of physical properties, which provide different values of $Q_{\min}$ within a synthetic reservoir layer (Table 3). However, for all simulations $Q_{\min}$ occurs at $f_{tr} = 6.5$ Hz. The synthetic reservoir rock corresponds to sandstone partially saturated with water and gas (Table 2). To quantify the reflection coefficient of such reservoir layer with attenuation caused by interlayer flow, we used the model setup shown in Figure 5. The source is a sinusoidal signal with a frequency of 6.5 Hz and the receiver is located close to the top of the synthetic reservoir. The thin layer is located at a distance of 2.8 times the wavelength of the sinusoidal signal. The background medium is effectively elastic, achieved by setting $\phi = 0.01$ for the poroelastic model. We want to quantify the impact of only attenuation on the reflection coefficient without any contrast in the real part of the acoustic impedance.

Table 3. Parameter variation for the reflection simulations (Figure 5). The permeability k is changed to locate Q_{min} in all simulations at 6.5 Hz; λ is the wavelength in the background medium at that frequency.

c	38	28	20	14	10	7	5
k (mD)	170	152	138	125	117	110	105
Q_{min}	4.2	5.0	6.2	8.1	10.7	14.7	20.2
λ (m)	535	504	464	427	389	354	324

Therefore, we set for each simulation the impedance of the background medium (having no attenuation) to the same value as the real part of the impedance of the reservoir layer at the transition frequency (which is also the frequency of the incident wave). This is done by only changing the density of the background medium. We use the analytical solution of the interlayer-flow model to determine the real part of the impedance of the reservoir (i.e., impedance caused by the real part of velocity V_P in equation 2).

We model the wave propagation in poroelastic and equivalent viscolastic media using an explicit finite-difference scheme that is second-order accurate both in time and space. For the porolastic simulations we use the partition method (Carcione and Quiroga-Goode, 1995) to solve Biot's equations (Biot, 1962). We successfully tested the scheme versus White's analytical solution (Quintal et al., 2007). For the viscoelastic simulations we use the standard linear solid model (Zener, 1948; Carcione, 2007) to simulate equivalent attenuation in the viscoelastic reservoir as described in equations 32–37.

For the poroelastic simulations, the reservoir consists of 104 periodically alternating couples of gas- and water-saturated layers, each couple being 48-cm thick providing a reservoir thickness of about 50 m. The optimal patch-size ratio (or saturation ratio), which provides the value of Q_{min}, is determined with equation 26. In our simulations with gas- and water-saturated sandstone about 9% of gas saturation (i.e., 4.32-cm thick gas-saturated layer) yields the lowest value of Q_{min}. We used 16 numerical nodes for the thinner layer (the gas-saturated layer) and 32 nodes for the thicker layer (the water-saturated layer), i.e., 2496 nodal points in the reservoir. In the viscoelastic case, the reservoir is a homogeneous solid and significantly less nodal points (200 nodal points) were required. The 50-m thick reservoir is considered a thin layer when compared to the wavelength in the background medium λ (Table 3). For our seven experiments the wavelength λ varies between 6.5 and 10.7 times the reservoir thickness.

To numerically quantify the absolute value of the reflection coefficient and the phase shift, we performed additional simulations in identical setups, but without the reservoir. For each experiment with a different parameter set, first we subtract the amplitude of the recorded particle velocity field of the simulation with reservoir from the one without reservoir (to remove the direct field, leaving only the reflected field), and second we divide the difference in amplitude by the amplitude of the original incident particle velocity field to obtain the absolute value of the reflection coefficient. To obtain the respective phase shifts between the reflected and incident signals, we measure the time shift in two different ways, and average them to reduce the effect of distortion in the shape of the reflected signal. One way was to measure the shift between the first maxima of reflected and incident signals; the other way was to use in each signal the first zero point after the first maximum as reference. The phase shift is proportional to the time shift.

We also analytically calculate the absolute value of the reflection coefficient and the phase shift, using a 1D analytical solution for the complex, frequency-dependent, reflection coefficient of an elastic layer embedded in an elastic background medium given by (e.g., Brekhovskikh, 1980)

$$R = \frac{1 - z}{1 + z}\left(1 - \frac{4zu}{(1 + z)^2 - u(1 - z)^2}\right), \qquad (38)$$

where $u = \exp(-i2h\omega/V_2)$, h is the thickness of the layer (i.e., the reservoir thickness), and $z = V_2\rho_2/V_1\rho_1$ is the elastic impedance ratio. Index 2 represents the layer, and index 1 represents the background medium. To account for the attenuation within the layer we use the complex P-wave velocity given by White's analytical solution (V in equation 3) for V_2 in equation 38. The reflection coefficient is complex and its magnitude is the absolute value of R. The phase

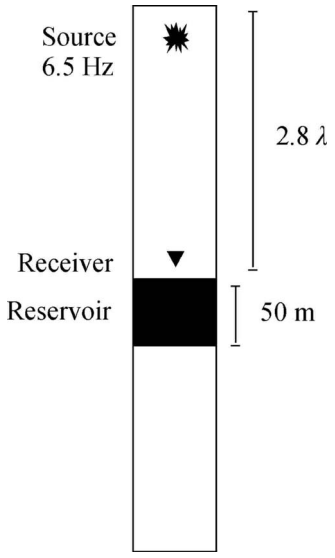

Figure 5. Model setup for numerical reflection simulations. The background medium above and below the reservoir layer is effectively elastic and the reservoir is either partially saturated poroelastic or viscoelastic. The parameters used in the simulations are given in Tables 2 and 3. The wavelength in the background medium λ is different in each simulation (Table 3) due to a different set of parameters. The density of the background medium is always changed in such a way so there is no elastic (real part of) impedance contrast between the reservoir and the background medium. The reservoir depth is set to be a function of the wavelength in the background medium so each wave always travels the same distance in terms of wavelength (here 2.8 λ) from the receiver to the upper boundary of the reservoir.

shift, associated with the reflection coefficient, is given by

$$\Psi = \tan^{-1}\frac{\mathrm{Im}(R)}{\mathrm{Re}(R)}. \quad (39)$$

Figure 6 shows the numerical and analytical results for the absolute value of the reflection coefficient (Figure 6a) and the phase shift (Figure 6b) as a function of $Q_{\min}$ within the layer. We observe that the absolute value of the reflection coefficient increases with increasing attenuation (decreasing Q) within the layer, and the numerical results for poroelastic and equivalent viscoelastic media agree well with the analytical results. Changing the quality factor by a factor of five changes the absolute value of the reflection coefficient by about a factor of eight. The difference, in the absolute value of the reflection coefficient and the phase shift, between the numerical results for the poroelastic simulation and the analytical results can be up to 25% (when $Q_{\min} = 20.2$). However, the analytical results are not the result for the same mathematical model describing interlayer flow in poroelastic solids, which was solved with finite differences. Therefore, the difference between analytical and numerical results here does not represent a numerical error, but rather the difference between the analytical approximation and the full numerical solution.

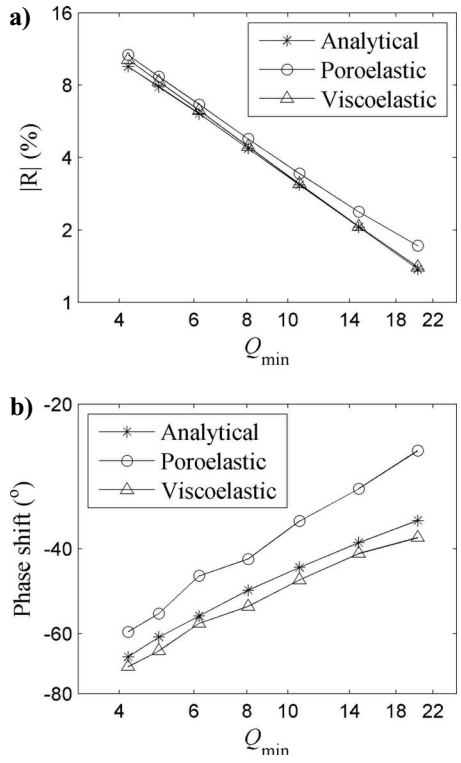

Figure 6. (a) Absolute value of the reflection coefficient of the 50-m thin layer (Figure 5) and (b) the associated phase shift versus the minimum value of quality factor $Q_{\min}$ within the layer. All axes are in logarithmic scale. Different values of $Q_{\min}$ have been generated by varying the value of c (see Table 3). The reflection is only caused by a contrast in attenuation. Changing the quality factor by a factor of five changes the absolute value of the reflection coefficient by about a factor of eight. The reflection coefficient can be as high as 10% for a value the of Q of about four. The absolute value of the reflection coefficient and phase shift have been calculated using an analytical solution (equation 38), and numerical simulations of wave propagation in both a partially saturated poroelastic medium and the equivalent viscoelastic medium. The absolute values and the slope of the relation between the reflection coefficient and the quality factor agree well for all three models. The same is observed for the phase shift. The maximal difference, in both the reflection coefficient and phase shift, between the numerical interlayer-flow solution (poroelastic) and the simple analytical solution is about 25% (when $Q_{\min} = 20.2$).

DISCUSSION

In this study we only considered interlayer flow caused by differences in the properties of the two pore fluids. For partial water/gas saturation, the highest attenuation occurs for a small amount of gas (about 9% saturation). We derived a new approximation for the patch-size or saturation ratio (equation 26), which enables calculating the water and gas saturations providing the minimum value of the quality factor. We expect that this approximation is also valid for other combinations of pore fluids, such as partial water/oil or oil/gas saturation, because $Q_{\min}$ can always be approximated as a linear function of $g_1 + g_2$, and only the values of the coefficients in equation 21 are expected to vary with different pore fluids.

At the transition frequency, the phase velocities predicted by the Gassmann-Wood and Gassmann-Hill limits exhibit the largest difference, which means the largest dispersion and the largest attenuation (or minimum quality factor). Attenuation caused by interlayer flow can also occur if the two fluid properties are identical but the properties of the rock alternate periodically, such as for example the grain bulk modulus or the porosity (e.g., Pride et al., 2004). For realistic petrophysical parameters the variations of pore fluid bulk modulus and porosity most likely generate the highest values of attenuation (Carcione and Picotti, 2006).

The reflection coefficient from the thin layer with attenuation (Figure 6) is also affected by tuning. The applied layer thickness is between six to 11 times smaller than the wavelength of the incident wave and therefore smaller than the tuning thickness, which is four times smaller than the wavelength (e.g., Brekhovskikh, 1980; Kallweit and Wood, 1982). This means that the reflection coefficient can even be larger if the layer thickness corresponds to the tuning thickness. In addition, the slope of the curve reflection coefficient versus Q (Figure 6a) is also affected by tuning because the layer becomes relatively thicker compared to the wavelength of the incident wave for increasing values of Q (Table 3).

The observed increased reflectivity of hydrocarbon reservoirs at low frequencies (e.g., Goloshubin et al., 2006) can be caused by wave-induced fluid flow resulting from partial gas saturations at the mesoscopic scale. Zones of small gas saturation and high attenuation may be located around the hydrocarbon reservoir at the water/gas or oil/gas contacts where the saturation changes gradually. Low-frequency reflections could be promising also for 4D (time-lapse) monitoring purposes, for example, to localize the gas/water front or to monitor changes in the gas saturation through the corresponding change in attenuation and, hence, reflectivity.

Numerical modeling of wave propagation in a poroelastic partially saturated (or patchy saturated) medium requires very high spatial resolution because every patch has to be numerically resolved accurately. An equivalent viscoelastic model, such as the one presented here, can be very useful for 2D and 3D numerical simulations in poroelastic partially saturated media with complicated geometries. Our simple viscoelastic model provides a good approximation to the interlayer-flow model for frequencies lower than and around the transition frequency (Figure 4).

CONCLUSIONS

We derived a simple approximation for the minimum value of the quality factor, Q_{min}, of the interlayer-flow model. The approximation provides accurate results for realistic values of parameters for sandstones partially saturated with water and gas. We also derived the optimal saturation ratio (or patch-size ratio) as a function of the elastic moduli and the porosity, which provides the smallest value of Q. The interlayer-flow model can provide values of Q as small as 2 for realistic values of petrophysical parameters for sandstones partially saturated with gas and water.

We presented a simple equivalent viscoelastic model for the interlayer-flow model, which can be used when the maximum frequency of the bandwidth of the numerical simulation is less than about four times the transition frequency (frequency at which Q_{min} occurs).

We showed that the analytical solution for the reflection coefficient of a thin elastic layer embedded in an elastic medium can be used to estimate the reflection coefficient from a thin partially saturated poroelastic layer with high attenuation caused by interlayer flow.

The contrast only resulting from attenuation between a thin layer (thickness $\ll$ wavelength) with attenuation (caused by interlayer flow) and a background medium without attenuation can yield significant reflections. High attenuation (e.g., $Q \approx 4$) in thin layers can lead to high reflection coefficients ($R \approx 10\%$) in the low-frequency range ($f_{tr} \approx 6.5$ Hz).

ACKNOWLEDGMENTS

These results have been obtained thanks to the support of the ETH Zurich. This research was cofinanced by KTI/CTI (The Innovation Promotion Agency in Switzerland) and Spectraseis. We thank Ken Larner, Brad Artman, and Erik H. Saenger for very helpful comments and suggestions. Comments by three reviewers, an associate editor, and the assistant editor, José Carcione, are greatly appreciated.

REFERENCES

Biot, M. A., 1962, Mechanics of deformation and acoustic propagation in porous media: Journal of Applied Physics, **33**, 1482–1498.

Bourbié, T., O. Coussy, and B. Zinszner, 1987, Acoustics of porous media: Editions Technip.

Bourbié, T., and A. Gonzalez-Serrano, 1983, Synthetic seismograms in attenuating media: Geophysics, **48**, 1575–1587.

Bourbié, T., and A. Nur, 1984, Effects of attenuation on reflections: Experimental test: Journal of Geophysical Research, **89**, 6197–6202.

Brekhovskikh, L. M., 1980, Waves in layered media: Academic Press.

Cadoret, T., G. Mavko, and B. Zinszner, 1995, Influence of frequency and fluid distribution effect on elastic wave velocities in partially saturated limestones: Journal of Geophysical Research, **100**, 9789–9803.

———, 1998, Fluid distribution effect on sonic attenuation in partially saturated limestones: Geophysics, **63**, 154–160.

Carcione, J. M., 2007, Wave fields in real media: Wave propagation in anisotropic, anelastic, porous and electromagnetic media: Elsevier, Handbook of Geophysical Exploration **38**, 4.

Carcione, J. M., H. B. Helle, and T. Zhao, 1998, Effects of attenuation and anisotropy on reflection amplitude versus offset: Geophysics, **63**, 1652–1658.

Carcione, J. M., and S. Picotti, 2006, P-wave seismic attenuation by slow-wave diffusion: Effects of inhomogeneous rock properties: Geophysics, **71**, no. 3, O1-O8.

Carcione, J. M., and G. Quiroga-Goode, 1995, Some aspects of the physics and numerical modeling of Biot compressional waves: Journal of Computational Acoustics, **3**, 261–280.

Chapman, M., E. Liu, and X. Li, 2006, The influence of fluid-sensitive dispersion and attenuation on AVO analysis: Geophysical Journal International, **167**, 89–105.

Dasgupta, R., and R. A. Clark, 1998, Estimation of Q from surface seismic reflection data: Geophysics, **63**, 2120–2128.

Dutta, N. C., and H. Odé, 1979a, Attenuation and dispersion of compressional waves in fluid-filled porous rocks with partial gas saturation (White model) — Part II: Results, Geophysics, **44**, 1777–1788.

———, 1979b, Attenuation and dispersion of compressional waves in fluid-filled porous rocks with partial gas saturation (White model) — Part II: Results, Geophysics, **44**, 1789–1805.

Dutta, N. C., and A. J. Seriff, 1979, On White's model of attenuation in rocks with partial gas saturation: Geophysics, **44**, 1806–1812.

Ganley, D. C., 1981, A method for calculating synthetic seismograms which include the effects of absorption and dispersion: Geophysics, **46**, 1100–1107.

Goloshubin, G., C. Van Schuyver, V. Korneev, D. Silin, and V. Vingalov, 2006, Reservoir imaging using low frequencies of seismic reflections: The Leading Edge, **25**, 527–531.

Kallweit, R. S., and L. C. Wood, 1982, The limits of resolution of zero-phase wavelets: Geophysics, **47**, 1035–1046.

Klimentos, T., 1995, Attenuation of P- and S-waves as a method of distinguishing gas and condensate from oil and water: Geophysics, **60**, 447–458.

Korneev, V. A., G. M. Goloshubin, T. M. Daley, and D. B. Silin, 2004, Seismic low-frequency effects in monitoring fluid-saturated reservoirs: Geophysics, **69**, 522–532.

Krief, M., J. Garat, J. Stellingwerff, and J. Ventre, 1990, A petrophysical interpretation using the velocities of P and S waves (full waveform sonic): The Log Analyst, **31**, 355–369.

Liu, H. P., D. L. Anderson, and H. Kanamori, 1976, Velocity dispersion due to anelasticity; Implications for seismology and mantle composition: Geophysical Journal of the Royal Astronomical Society, **47**, 41–58.

Maultzsch, S., M. Chapman, E. Liu, and X. Y. Li, 2003, Modelling frequency-dependent seismic anisotropy in fluid-saturated rock with aligned fractures: Implication of fracture size estimation from anisotropic measurements: Geophysical Prospecting, **51**, 381–392.

Mavko, G., T. Mukerji, and J. Dvorkin, 1998, The rock physics handbook: Tools for seismic analysis in porous media: Cambridge University Press.

Müller, T. M., and B. Gurevich, 2005, Wave-induced fluid flow in random porous media: Attenuation and dispersion of elastic waves: Journal of the Acoustical Society of America, **117**, 2732–2741.

Murphy, W. F., 1984, Acoustic measures of partial gas saturation in tight sandstones: Journal of Geophysical Research, **89**, 11549–11559.

Norris, A. N., 1993, Low-frequency dispersion and attenuation in partially saturated rocks: Journal of Acoustical Society of America, **94**, 359–370.

Pride, S. R., 2003, Relationships between seismic and hydrological properties, *in* Y. Rubin and S. Hubbard eds., Hydrogeophysics: Springer, 253–290.

Pride, S. R., J. G. Berryman, and J. M. Harris, 2004, Seismic attenuation due to wave-induced flow: Journal of Geophysical Research **109**, B01201, doi: 10.1029/2003JB002639.

Quintal, B., S. M. Schmalholz, Y. Y. Podladchikov, and J. M. Carcione, 2007, Seismic low-frequency anomalies in multiple reflections from thinly-layered poroelastic reservoirs: 77th Annual International Meeting, SEG, Expanded Abstracts, 1690–1695.

Rapoport, M. B., L. I. Rapoport, and V. I. Ryjkov, 2004, Direct detection of oil and gas fields based on seismic inelasticity effect: The Leading Edge, **23**, 276–278.

Toms, J., T. M. Mueller, R. Ciz, and B. Gurevich, 2006, Comparative review of theoretical models for elastic wave attenuation and dispersion in partially saturated rocks: Soil Dynamics and Earthquake Engineering, **26**, 548–565.

White, J. E., 1975, Computed seismic speeds and attenuation in rocks with partial gas saturation: Geophysics, **40**, 224–232.

White, J. E., N. G. Mikhaylova, and F. M. Lyakhovitskiy, 1975, Low-frequency seismic waves in fluid saturated layered rocks: Izvestija Academy of Sciences USSR, Physics of the Solid Earth, **11**, 654–659.

Zener, C., 1948, Elasticity and anelasticity of metals: University of Chicago Press.